Improved Mathematical Model of PMSM Taking Into Account Cogging Torque Oscillations

Tiberiu TUDORACHE, Ion TRIFU, Constantin GHITA, Valeriu BOSTAN
Politehnica University of Bucharest, 060042, Romania

***Abstract*—This paper presents an improved mathematical model of Permanent Magnet Synchronous Machine (PMSM) that takes into account the Cogging Torque (CT) oscillations that appear due to the mutual attraction between the Permanent Magnets (PMs) and the anisotropic stator armature. The electromagnetic torque formula in the proposed model contains an analytical expression of the CT calibrated by Finite Element (FE) analysis. The numerical calibration is carried out using a data fitting procedure based on the Simplex Downhill optimization algorithm. The proposed model is characterized by good accuracy and reduced computation effort, its performance being verified by comparison with the classical d-q model of the machine using Matlab/Simulink environment.**

***Index Terms*—finite element methods, mathematical model, numerical simulation, optimization, permanent magnet machines.**

I. INTRODUCTION

The Permanent Magnet Synchronous Machine (PMSM) is an electromechanical converter frequently used in industry, especially in small power applications, due to its specific advantages, such as: high efficiency, lack of sliding contacts, high energy density per volume unit, safe operation, fast and accurate speed response etc. Modern applications where PMSM is competitive are numerous, some examples referring to: servo drive systems, electric or hybrid electric vehicles, small to medium power wind turbines, etc. [1]-[7]. Several aspects related to the optimal design and operation of PMSM were studied, some of them referring to demagnetization faults of Permanent Magnets (PMs) [8], multilevel optimal design [9], analytical models for rapid analysis [10], losses evaluation techniques [11], cogging torque reduction methods [12], [13] etc.

Despite its attractiveness, PMSM has a main drawback represented by the presence of the Cogging Torque (CT) that appears due to the mutual attraction between the PMs and the stator teeth [12], [13]. CT can also be explained by the variation of the magnetic energy in the machine air-gap with respect to the rotor/stator relative position.

CT produces only negative effects in electrical machines because it does not contribute to the net active torque of electrical motors or to the resistant (antagonist) electromagnetic torque of electrical generators, because its mean value on a period is null. The phenomena caused by CT that disturb the PMSM operation are: noise and vibrations that increase the mechanical losses [14]-[16], increase of cut-in speed of wind turbines [17], [18], precision reduction in case of positioning systems [19] etc.

The problems related to the CT are particularly important for low speed high torque wind PMSM generators (direct drive type), since CT may reach important peak values that may prevent the turbines to produce electricity at small wind speeds, reducing thus their efficiency [17], [18]. Despite the importance of CT, in many cases, the numerical analysis of the transient regimes of PMSM is based on several simplifying hypothesis that neglect its presence [20].

The most adequate mathematical models for the transient analysis of PMSM in general should meet two main criteria, i.e. high accuracy and reasonable computation effort.

The most common numerical model used for the analysis of the transient regimes of PMSM, that perform very well in terms of computation effort, is the d-q orthogonal model. This is a lumped parameters model, based on the voltage equations of the machine written in the orthogonal d-q coordinates system [20]- [22]. The main disadvantage of this model is the lack of accuracy that derives from the simplifying hypothesis that the model relies on.

A numerical model more and more used in the last decades for the analysis of transient regimes of PMSM is based on Finite Element Method (FEM), generally in 2D approach. This is a laborious model, characterized by high accuracy and by the capability of taking into account complex phenomena such as cogging torque, teeth harmonics, etc. [23]. An important drawback of this model is related to the huge computation effort. The computation burden increases dramatically when the analyzed electrical machine is integrated in a PWM drive system since the integration time step should be correlated with the commutation frequency [24].

The mathematical model of the PMSM proposed in this paper is a modified d-q orthogonal model able to take into account the CT oscillations as a component of the electromagnetic torque. This complex model combines the advantages of the two models described above, offering more accurate results in terms of electromagnetic torque compared to the common d-q model of PMSM.

The physical support for this study is a small power PMSM characterized by the main data presented in Table I.

TABLE I. MAIN DATA OF THE STUDIED PMSM AS GENERATOR

Rated power [W]	Rated speed [rpm]	No. of poles	Stator bore diam. [mm]	Stator outer diam. [mm]	Axial length [mm]	No. of slots
400	1800	12	90	128	15	36

The work has been co-funded by the Sectoral Operational Programme Human Resources Development 2007-2013 of the Romanian Ministry of Labour, Family and Social Protection through the Financial Agreements POSDRU/89/1.5/S/62557 and POSDRU/107/1.5/S/76909.

Digital Object Identifier 10.4316/AECE.2012.03009

The Permanent Magnets (PMs) mounted on the circular rotor outer surface are chamfered so as to obtain an e.m.f. waveform close to a perfect sine wave. The machine air-gap being constant, the longitudinal and transversal inductivities are equal with the synchronous inductance:

$$L_s = L_d = L_q \tag{1}$$

II. Analytical CT Model

The CT can be computed by the derivative of magnetic energy W produced by the PMs with respect to the rotor mechanical position angle α:

$$T_c(\alpha) = -\left.\frac{\partial W}{\partial \alpha}\right|_{\Phi=const.} \tag{2}$$

Neglecting the magnetic saturation of magnetic cores and the end effect, the expression of CT can be decomposed in Fourier Series as follows [25]:

$$T_c(\alpha) = \sum_{k=1}^{\infty} T_k \sin(kZ\alpha + \varphi_k) \tag{3}$$

where Z is the number of stator slots, and T_k and φ_k are the amplitude and phase shift of harmonic number k respectively.

A good approximation of the T_c may use only four terms (k = 1 … 4) of the Fourier Series decomposition (3), while the unknown values of T_k and φ_k in (3) could be computed using FE analysis.

III. FEM Computation of CT

The precise evaluation of CT can be done using a 2D parallel-type FE computation model of the PMSM. The computation domain is represented by a cross section through the machine, Fig. 1. The finite element discretization of the computation domain consists of around 38000 second order triangular elements with smaller size in the air-gap region where the most part of the magnetic energy is concentrated, Fig. 1. Three layers of finite elements were used in the air-gap region to ensure a good computation accuracy of CT.

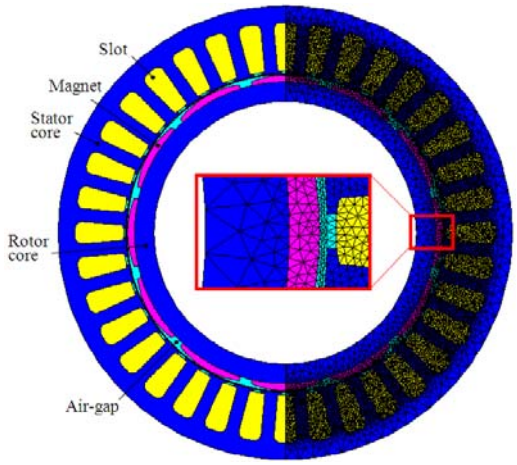

Figure 1. Cross section through the studied PMSM; FE computation domain, main regions and mesh.

The computation of CT oscillations is based on a series of 2D magneto-static field computations governed by the following partial differential equation:

$$\nabla \times \left[\frac{1}{\mu}\nabla \times \boldsymbol{A}\right] = \nabla \times \left[\frac{1}{\mu}\boldsymbol{B}_r\right] \tag{4}$$

where $\boldsymbol{A}$ is the magnetic vector potential, μ is the magnetic permeability of materials, $\boldsymbol{B}_r$ the remnant flux density of permanent magnets.

The stator magnetic core of the PMSM is made of standardized magnetic steel laminations M600-50A and the rotor core is made of regular steel. The permanent magnets are made of NdFeB N35 type, with a remnant magnetic flux density B_r = 1.195 T and μ_r = 1.037.

The magnetic field lines and the chart of the magnetic flux density obtained by solving the 2D magneto-static field problem for a given relative stator/rotor position are shown in Fig. 2.

The oscillations of CT are computed by successive 2D magneto-static simulations for different stator/rotor relative positions, using the Virtual Works Method, Fig. 3. The peak value of CT is about 0.2 Nm, representing about 9.5% of the rated torque evaluated at about 2.1 Nm.

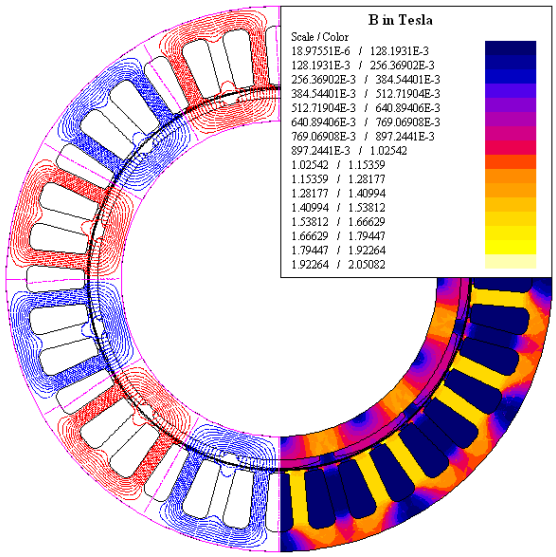

Figure 2. FE results; magnetic field lines and flux density chart.

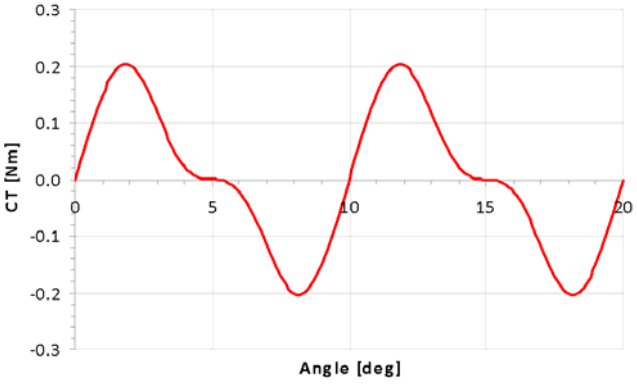

Figure 3. CT oscillations versus stator/rotor relative position angle (FEM).

IV. Calibration of Analytical Model of CT

The calibration of the analytical model of CT is based on the expression (3) where the coefficients T_k and φ_k are determined so as the analytical curve fits as well as possible the FEM computed curve of CT shown in Fig. 3.

The data fitting operation, whose diagram is presented in Fig. 4, aims at finding the most suitable coefficients T_k and φ_k that minimize the sum of squared residuals. The residuals represent the differences between the FEM computed CT data and the analytical ones. The optimization algorithm used in the data fitting procedure is a modified Simplex Downhill algorithm with several restarts from different initial guess points.

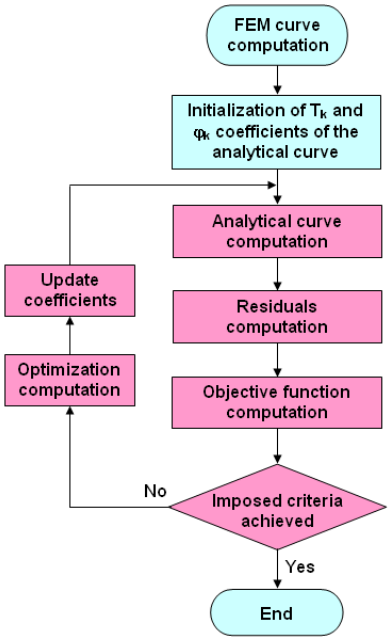

Figure 4. Data fitting procedure based on optimization algorithm, used to determine the coefficients T_k and φ_k.

After successive computations the best T_k and φ_k coefficients found for the first 4 harmonics, shown in Table II, lead to the CT analytical curve presented in comparison with the FEM computed CT curve in Fig. 5. The two curves are practically superposed.

TABLE II
Optimal Coefficients T_k [Nm] and φ_k [rad]

T_1	φ_1	T_2	φ_2	T_3	φ_3	T_4	φ_4
0.162	0.009	0.068	0.010	-0.010	0.017	-0.002	0.017

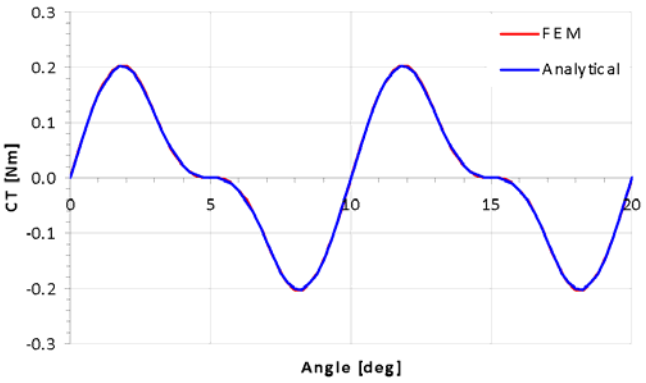

Figure 5. Analytical and FEM computed CT curves.

Thus the analytical expression of the CT as a function of the rotor/stator angular position α, resulted from the data fitting operation, is as follows:

$$T_c(\alpha) = \sum_{k=1}^{4} T_k \sin(36k\alpha + \varphi_k) \tag{5}$$

where T_k and and φ_k are shown in Table II.

V. Implementation of Improved d-q Model of PMSM

A. Equations of the improved d-q model of PMSM

The general equations expressed in the rotor reference frame that define the classical d-q model of the PMSM working as motor are the following:

$$\begin{cases} \dfrac{di_d}{dt} = \dfrac{v_d}{L_d} - \dfrac{Ri_d}{L_d} + \dfrac{L_q}{L_d} p\omega_r i_q \\ \dfrac{di_q}{dt} = \dfrac{v_q}{L_q} - \dfrac{Ri_q}{L_q} - \dfrac{L_d}{L_q} p\omega_r i_d - \Phi \dfrac{p\omega_r}{L_q} \\ T_e = \dfrac{3}{2} p\left[\Phi i_q + \left(L_d - L_q\right) i_d i_q\right] \\ \dfrac{d\omega_r}{dt} = \dfrac{1}{J}\left(T_e - F\omega_r - T_m\right) \end{cases} \tag{6}$$

where i_d and i_q are the d and q axis stator currents, L_d and L_q are the d and q axis inductances, v_d and v_q are d and q axis stator voltages, R is the phase resistance, p is the number of pole pairs, ω_r is the rotor angular speed, Φ is the amplitude of the magnetic flux created by the PMs, T_e is the electromagnetic torque that neglects CT, J is the combined moment of inertia of rotor and load, F is the combined viscous friction coefficient of rotor and load and T_m is the shaft mechanical torque. These equations are based on several simplifying hypothesis that neglect the existence of CT oscillations [21].

The particular construction of the studied PMSM with constant air-gap implies that the inductances L_d and L_q in (6) are equal with the synchronous inductance L_s.

The improved d-q model of the PMSM supposes to modify the expression of electromagnetic torque T_e in (6), by adding the CT component, T_c. The expression of the resulting electromagnetic torque T_e' becomes:

$$T_e' = T_e + T_c \tag{7}$$

Since the expression of CT depends on rotor/stator angular position α, this angular coordinate should be computed at each time step during the simulation process.

B. PMSM parameters computation using a FEM analysis

The implementation of the d-q model for the studied PMSM supposes first to compute all the necessary parameters appearing in (6). In our case the phase resistance is already known, R = 0.3 Ω, but the inductance $L_s = L_d = L_q$ and the amplitude of the magnetic flux Φ are unknown and they should be determined from the FEM model of the machine.

The computation of the synchronous inductance L_s can be

done starting from the PMSM voltage phasor diagram per phase, for the machine working as generator, as shown in Fig. 6 a). In this diagram, V represents the voltage per phase at the machine terminals and $X_s = p\omega_r L_s$ is the synchronous reactance. In case of purely resistive load, the voltage phasor diagram looks like in Fig. 6 b).

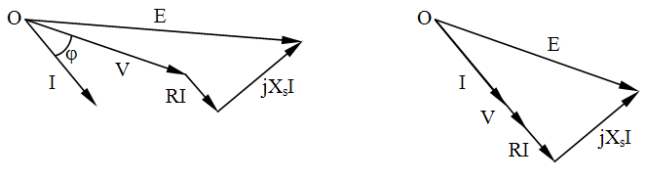

a) b)

Figure 6. PMSM voltage phasor diagram per phase; a) general phasor diagram; b) phasor diagram for a resistive load.

In case of resistive load if we apply Pythagoras Theorem for the right-angled triangle shown in Fig. 6 b), we can write:

$$X_s = \frac{\sqrt{E^2 - (V + RI)^2}}{I} \tag{8}$$

In order to compute the synchronous inductance L_s from (8), a FEM transient magnetic analysis of the PMSM is necessary, with the rotor moving at the rated angular speed ω_r.

In order to easily compute the quantities E, V and I the FEM model of PMSM was coupled with the associated circuit model shown in Fig. 7.

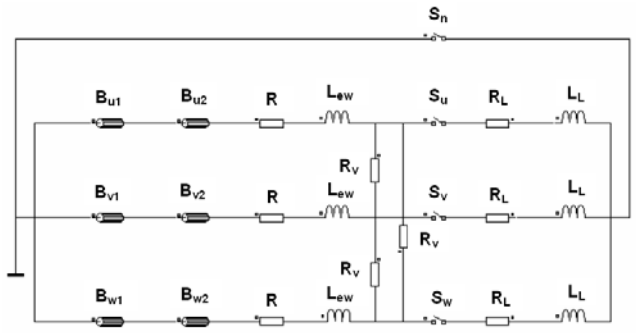

Figure 7. Circuit model associated to the FEM model of PMSM.

The circuit components of the electric diagram shown in Fig. 7 are the following: R - stator phase resistance, B_{u1}, B_{u2}, ... B_{w2} - positively and negatively oriented coil sides of stator windings (156 turns per phase), L_{ew} - end winding inductances (L_{ew} = 1 mH), R_v - voltmeters, S_u, S_v, S_w, S_n - switches, R_L - load resistances, L_L - load inductances (useful for modeling R-L loads).

In order to compute the e.m.f., a FEM transient magnetic analysis of the PMSM was carried out, in no load regime (this regime was simulated by imposing a very high value for the load resistances R_L in the circuit shown in Fig. 7). By this analysis, the voltage per phase computed at the machine terminals is equal with the e.m.f. ($V_0 = E$).

To compute the voltage V and current I for a purely resistive load, a FEM transient magnetic analysis of the PMSM should be done with the machine working as generator, with a resistive load coupled to its terminals (this regime is simulated by imposing in the circuit shown in Fig. 7 a very small value of the load inductance L_L and a proper value of the load resistance; in our case $R_L = 5\Omega$).

Another unknown quantity that appears in d-q model in (6) is the magnetic flux amplitude Φ. This quantity was computed (Φ = 0.0312 Wb) by fitting the peak voltage obtained by FEM transient magnetic analysis with the peak voltage obtained by the improved d-q model.

The numerical data obtained by the FEM transient magnetic analysis of PMSM working as generator, are presented in Table III.

TABLE III
DATA OBTAINED BY THE FEM TRANSIENT MAGNETIC ANALYSIS

E [V]	V [V]	I [A]	X_s [Ω]	L_s [mH]	Φ [mWb]
24.92	21.74	4.332	2.187	1.934	31.16

VI. NUMERICAL RESULTS

A. PMSM used as generator driven by constant torque

The performance of the improved d-q model of PMSM is exemplified by integrating the model in a Simulink bloc diagram and using it to simulate the operation of the machine as generator driven by constant torque, delivering energy on a resistive load, Fig. 8.

The numerical results obtained for classical and for improved d-q model of the studied PMSM in steady state are presented comparatively in Fig. 9.

We can notice the presence of the CT oscillations in the wave form of the electromagnetic torque that involves also small oscillations of the rotor speed, unlike the classical d-q model where these oscillations do not exist.

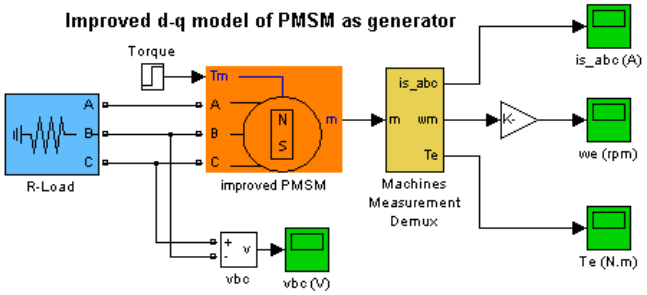

Figure 8. Simulink bloc diagram used to simulate the operation of PMSM as generator driven by constant torque.

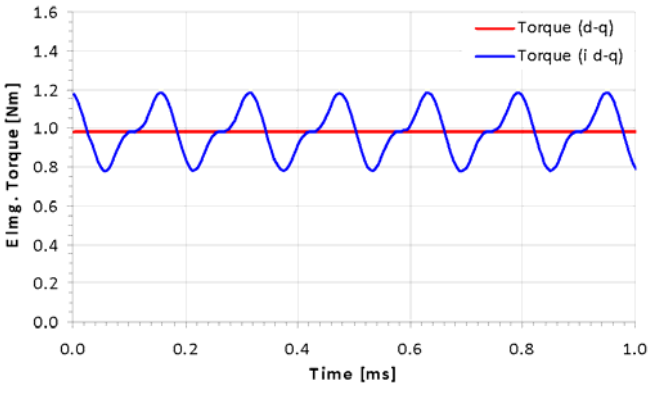

a)

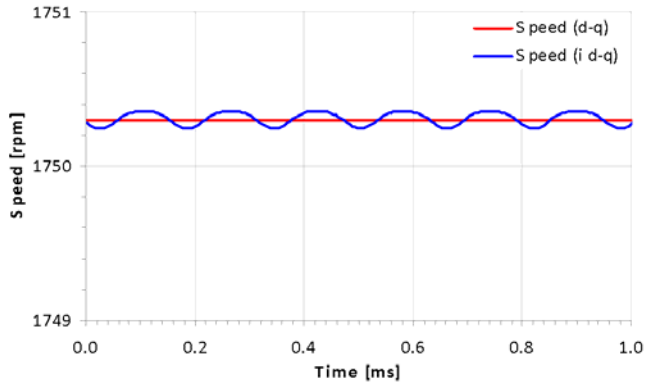

b)

Figure 9. Simulink numerical results in case of PMSM working as generator driven by constant torque ("d-q" means classical d-q model; "i d-q" means improved d-q model); a) Electromagnetic torque; b) Rotor speed.

These steady state results correspond to a viscous friction coefficient F = 0.0001 Nms and to a moment of inertia $J = 0.0007$ kg · m^2.

We should notice that in case of PMSM with high CT peak values and small moment of inertia the speed oscillations could be much more pronounced.

B. PMSM working as motor under load condition

The improved d-q model of PMSM working as motor, integrated in the Simulink bloc diagram shown in Fig. 10, leads to the numerical results shown in Fig. 11 in comparison with those obtained by the classical d-q model of the machine.

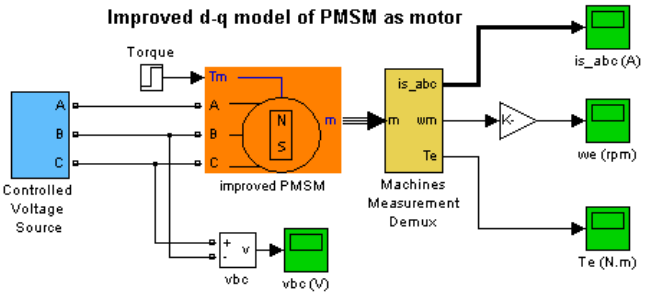

Figure 10. Simulink bloc diagram used to simulate the operation of PMSM as motor under load condition.

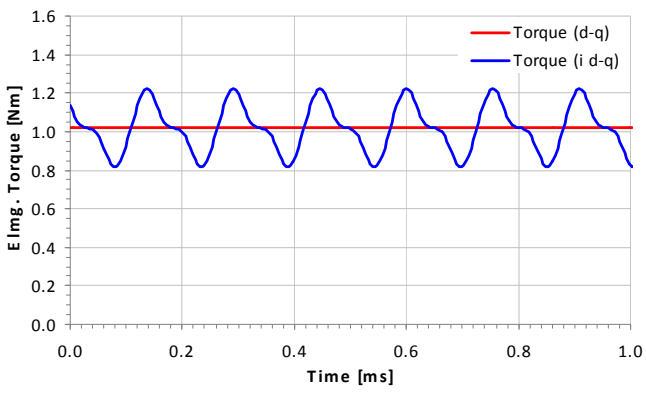

a)

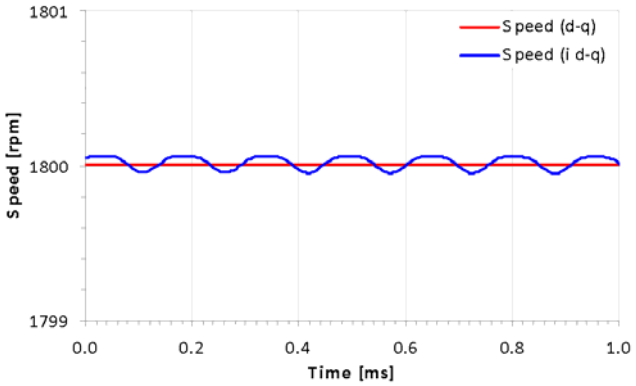

b)

Figure 11. Simulink numerical results in case of PMSM working as motor ("d-q" means classical d-q model; "i d-q" means improved d-q model); a) Electromagnetic torque; b) Rotor speed.

We can notice the presence of CT oscillations in the wave form of the electromagnetic torque of the PMSM that involves small speed oscillations that practically do not exist in case of the classical d-q model.

VII. CONCLUSION

This paper presents an improved d-q model of the PMSM able to take into account the CT oscillations specific to this type of machine.

The proposed mathematical model characterized by a good trade-off between high accuracy and low computation effort is very useful for the transient analysis of the PMSM. The elaboration of this model requires first a series of three FEM transient magnetic analyses for the computation of a list of requires quantities such as: CT oscillations, e.m.f., phase voltage and phase current, magnetic flux amplitude. Once elaborated, the model can be successfully used in complex drive schemes offering good precision numerical results in short computation time.

The simulation results obtained for the studied PMSM operated as motor and generator emphasize the ability of the proposed model, in contrast with the classical d-q model of the machine, to take into account the CT oscillations and their effects, being thus a valuable tool that can be used to predict the operation features of PMSM.

REFERENCES

[1] B. Abdi, J. Milimonfared, J. Shokrollahi Moghani, A. Kashefi Kaviani, "Simplified Design and Optimization of Slotless Synchronous PM Machine for Micro-Satellite Electro-Mechanical Batteries", Advances in Electrical and Computer Engineering Journal, Vol. 9, No. 3, pp. 84-88, 2009. [Online]. Available: http://dx.doi.org/10.4316/aece.2009.03015

[2] S. Hosseini, J. S. Moghani, B. B. Jensen, "Accurate Modeling of a Transverse Flux Permanent Magnet Generator Using 3D Finite Element Analysis", Advances in Electrical and Computer Engineering Journal, Vol. 11, No. 3, pp. 115-120, 2011. [Online]. Available: http://dx.doi.org/10.4316/aece.2011.03019

[3] I. A. Viorel, L. Strete, K. Hameyer, "Construction and Design of a Modular Permanent Magnet Transverse Flux Generator", Advances in Electrical and Computer Engineering Journal, Vol. 10, No. 1, pp. 3-6, 2010. [Online]. Available: http://dx.doi.org/10.4316/aece.2010.01001

[4] T. Herold, E. Lange, K. Hameyer, "System Simulation of a PMSM Servo Drive Using Field-Circuit Coupling", *IEEE Trans. Magn.*, vol. 47, no. 5, 2011, pp. 938 - 941. [Online]. Available: http://dx.doi.org/10.1109/TMAG.2010.2090866

[5] B. Vaseghi, N. Takorabet, F. Meibody-Tabar, "Investigation of a Novel Five-Phase Modular Permanent-Magnet In-Wheel Motor",

IEEE Trans. Magn., vol. 47, no. 10, 2011, pp. 4084- 4087. [Online]. Available: http://dx.doi.org/10.1109/TMAG.2011.2150207

[6] P. Zheng, J. Zhao, R. Liu, C. Tong, Q. Wu, "Magnetic Characteristics Investigation of an Axial-Axial Flux Compound-Structure PMSM Used for HEVs", *IEEE Trans. Magn.*, vol. 46, no. 6, 2010, pp. 2191 - 2194. [Online]. Available: http://dx.doi.org/10.1109/TMAG.2010.2042042

[7] J. Sopanen, V. Ruuskanen, J. Nerg and J. Pyrhonen, "Dynamic Torque Analysis of a Wind Turbine Drive Train Including a Direct-Driven Permanent Magnet Generator", *Trans. Ind. Electron.*, vol. 58, no. 9, 2010, pp. 3859 - 3867. [Online]. Available: http://dx.doi.org/10.1109/TIE.2010.2087301

[8] J.-R.R. Ruiz, J.A. Rosero, A.G. Espinosa, L. Romeral, "Detection of Demagnetization Faults in Permanent-Magnet Synchronous Motors Under Nonstationary Conditions", *IEEE Trans. Magn.*, vol. 45, no. 7, 2009, pp. 2961 - 2969. [Online]. Available: http://dx.doi.org/10.1109/TMAG.2009. 2015942

[9] X. Meng, S. Wang, J. Qiu, Q. Zhang, J.G. Zhu, Y. Guo, D. Liu, "Robust Multilevel Optimization of PMSM Using Design for Six Sigma", *IEEE Trans. Magn.*, vol. 47, no. 10, 2011, pp. 3248 - 3251. [Online]. Available: http://dx.doi.org/10.1109/TMAG.2011.2157322

[10] Y. Wang, J. Zhu, Y. Guo, "A Comprehensive Analytical Mathematic Model for Permanent-Magnet Synchronous Machines Incorporating Structural and Saturation Saliencies", *IEEE Trans. Magn.*, vol. 46, no. 12, 2010, pp. 4081 - 4091. [Online]. Available: http://dx.doi.org/10.1109/TMAG.2010.2071392

[11] P. Sergeant, F. De Belie, L. Dupre, J. Melkebeek, "Losses in Sensorless Controlled Permanent-Magnet Synchronous Machines", *IEEE Trans. Magn.*, vol. 46, no. 12, 2010, pp. 4081 - 4091.

[12] G.H. Kang, Y.D. Son, G.T. Kim. J. Hur, "A Novel Cogging Torque Reduction Method for Interior-Type Permanent-Magnet Motor", *IEEE Trans. Magn.*, vol. 45, no. 1, 2009, pp. 161 - 167.

[13] D. Wang, X. Wang, Y. Yang and R. Zhang, "Optimization of Magnetic Pole Shifting to Reduce Cogging Torque in Solid-Rotor Permanent-Magnet Synchronous Motors", *IEEE Trans. Magn.*, vol. 46, no. 5, 2010, pp. 1228 - 1234. [Online]. Available: http://dx.doi.org/10.1109/TMAG.2010.2044044

[14] T. Sun, J.M. Kim, G.H. Lee, J.P. Hong, M.R. Choi, "Effect of Pole and Slot Combination on Noise and Vibration in Permanent Magnet Synchronous Motor", *IEEE Trans. Magn.*, vol. 47, no. 5, 2011, pp. 1038 - 1041. [Online]. Available: http://dx.doi.org/10.1109/TMAG.2010.2093872

[15] S.M. Hwang, J.B. Eom, G.B. Hwang, W.B. Jeong and Y.H. Jung, "Cogging torque and acoustic noise reduction in permanent magnet motors by teeth pairing", *IEEE Trans. Magn.*, vol. 36, no. 5, 2010, pp. 3144 - 3146. [Online]. Available: http://dx.doi.org/10.1109/20.908714

[16] Z.Q. Zhu, Y. Liu and D. Howe, "Minimizing the Influence of Cogging Torque on Vibration of PM Brushless Machines by Direct Torque Control", *IEEE Trans. Magn.*, vol. 42, no. 10, 2006, pp. 3512-3514. [Online]. Available: http://dx.doi.org/10.1109/TMAG.2006.879439

[17] E. Muljadi and J. Green, "Cogging Torque Reduction in a Permanent Magnet Wind Turbine Generator", *Proc. of the American Society of Mechanical Engineers Wind Energy Symposium*, Reno, Nevada, USA, 2002.

[18] T. Tudorache, L. Melcescu and M. Popescu, "Methods for Cogging Torque Reduction of Directly Driven PM Wind Generators", *Proc. of International Conference on Optimization of Electric and Electronic Equipment* (OPTIM 2010), Moieciu, Romania, 2010. [Online]. Available: http://dx.doi.org/10.1109/OPTIM.2010.5510390

[19] Hafner M., Franck D., Hameyer K., "Static Electromagnetic Field Computation by Conformal Mapping in Permanent Magnet Synchronous Machines", *IEEE Trans. Magn.*, vol. 46, no. 8, 2010, pp. 3105 - 3108. [Online]. Available: http://dx.doi.org/10.1109/TMAG.2010.2043930

[20] The Mathworks: "Permanent Magnet Synchronous Machine", Matlab & Simulink Help 2010.

[21] P. Pillay and R. Krishnan, "Modeling, Simulation and Analysis of Permanent-Magnet Motor Drives, Part I: The Permanent-Magnet Synchronous Motor Drive", *Trans. Ind. Appl.*, vol 25, no. 2, 1989, pp. 265 - 273. [Online]. Available: http://dx.doi.org/10.1109/28.25541

[22] D.Y. Ohm, "Dynamic Model of PM Synchronous Motors", Drivetech Inc., Blacksburg, Virginia, www.drivetech.com.

[23] M.A. Jabbar, Z. Liu and J. Dong, "Time stepping finite element analysis for the dynamic performance of a permanent magnet synchronous motor", *IEEE Trans. Magn.*, vol. 39, no. 5, 2003, pp. 2621 - 2623. [Online]. Available: http://dx.doi.org/10.1109/TMAG.2003.816500

[24] S. Brisset, T. Tudorache, P. Brochet and V. Fireteanu, "Finite element analysis of a brushless DC wheel motor with concentrated winding", *Proc. of International Aegean Conference on Electrical Machines and Power Electronics* (ACEMP 2007), Bodrum, Turkey, 2007. [Online]. Available: http://dx.doi.org/10.1109/ACEMP.2007.4510526

[25] N. Bianchi, S. Bolognani, "Design Techniques for Reducing the Cogging Torque in Surface-Mounted PM Motors", *IEEE Trans. Ind. Appl.*, vol. 38, no. 5, 2002, pp. 1259 - 1265. [Online]. Available: http://dx.doi.org/10.1109/TIA.2002.802989